International Journal of Pharmaceutics 379 (2009) 285–292

Contents lists available at ScienceDirect

International Journal of Pharmaceutics

journal homepage: www.elsevier.com/locate/ijpharm

Pharmaceutical Nanotechnology

Characterization of endocytosis of transferrin-coated PLGA nanoparticles by the blood–brain barrier

Jiang Chang[a,b,c], Youssef Jallouli[c], Maya Kroubi[a], Xu-bo Yuan[b], Wei Feng[b], Chun-sheng Kang[d], Pei-yu Pu[d], Didier Betbeder[a,c,*]

[a] EA 2689, Laboratory of Physiology, IMPRT, University of Lille 2, Faculté de Médecine, pôle recherche, 1 place de Verdun, 59045 Lille, France
[b] School of Materials Science and Engineering, Tianjin University, 300072 Tianjin, China
[c] EA 2648, Laboratory of Blood-Brain Barrier, IMPRT, University of Artois, Faculté des Sciences Jean Perrin, rue Jean Souvraz, 62307 Lens, France
[d] Department of Neurosurgery, Tianjin Medical University General Hospital, Laboratory of Neuro-oncology, Tianjin Neurological Institute, 300052 Tianjin, China

ARTICLE INFO

Article history:
Received 20 January 2009
Received in revised form 14 April 2009
Accepted 20 April 2009
Available online 3 May 2009

Keywords:
PLGA
Nanoparticles
blood–brain barrier
Transferrin
Caveolae

ABSTRACT

Many studies showed that transferrin increases brain delivery of nanoparticles (NPs) *in vivo*, however the mechanisms implied in their brain uptake are not yet clearly elucidated. In this study we evaluated the endocytosis of PLGA NPs coated with transferrin on an *in vitro* model of the blood–brain barrier (BBB) made of a *co*-culture of brain endothelial cells and astrocytes. PLGA NPs were prepared using DiI as a fluorescent marker and coated with Tween® 20, BSA and transferrin (Tf). Blank and BSA-NPs served as controls. The cellular toxicity on BBB of the different samples was evaluated following tight junction aperture and due to high toxicity NPs prepared with Tween® 20 were discarded. The size of the NPs prepared by the solvent diffusion method, varied from 63 to 90 nm depending on DiI incorporation and surface coating. Proteins adsorption on the surface of the NPs was found to be stable for at least 12 days at 37 °C. Contrary to Blank or BSA-NPs, Tf-NPs were found to be highly adsorbed by the cells and endocytosed using an energy-dependent process. Studies in presence of inhibitors suggest that Tf-NPs interact with the cells in a specific manner and enter the cells via the caveolae pathway.

1. Introduction

In the last few years, an increasing number of studies have been performed to develop efficient therapies for brain diseases such as cancers, HIV-dementia, strokes, ischemia, Alzheimer's and Parkinson's diseases (Hawkins and Davis, 2005; Ricci et al., 2006). These pathologies are particularly difficult to treat due to the presence of the blood–brain barrier (BBB), a vital element in the regulation of the internal environment of the brain which selectively allows the passage of desired molecules from the blood to the brain parenchyma (Edwards, 2001).

Among the various non-invasive approaches, nanoparticulate carriers and particularly polymeric nanoparticles (NPs) seem to be one of the most interesting strategies. These NPs are vectors with a 10–100 nm size and drugs can be loaded into the NPs, adsorbed or chemically linked to their surface. These carriers possess a higher stability in biological fluids and against the enzymatic metabolism than other colloidal carriers, such as the liposomes or lipidic vesicles (Huwyler et al., 1996).

Many attempts in using NPs as CNS drug delivery systems were performed with certain success (Blasi et al., 2007; Tosi et al., 2007), thus demonstrating the feasibility of drug delivery to the CNS by using these carriers. PBCA NPs coated with polysorbate 80 are able to cross BBB when administered intravenously (Ambruosi et al., 2006). Similar results were obtained in the presence of PEGylated polycyanoacrylate NPs (Calvo et al., 2001). PBCA NPs coated with polysorbate 80 were used to encapsulate dalargin, loperamide, NMDA-receptor antagonists and doxorubicin (Ambruosi et al., 2006). The mechanism of drug delivery across the BBB, with the surfactant-coated NPs appears to be due to adsorption of apolipoprotein E or A-1 after injection into the blood stream,

Abbreviations: BBB, blood–brain barrier; BCECs, bovine capillary endothelial cells; BSA, bovine serum albumin; BSA-NPs, BSA-coated nanoparticles; CNS, central nervous system; DiI, 1,1′-dioctadecyl 3′,3,3′,3′-tetramethylindo-carboxycyanate perchlorate; DMEM, Dulbecco's modified Eagle's medium; FITC, fluorescein isothiocyanate; FA, folic acid; HSA, human serum albumin; IGF, insulin-like growth factors; IL-1, interleukin-1; LDL, low density lipoprotein; LY, Lucifer Yellow; Mw, molecular weight; NMDA, N-methyl-D-aspartic acid; NPs, nanoparticles; γ-GT, γ-glutanyl transpeptidase; Tf, human holo-transferrin; Tf-NPs, transferrin-coated nanoparticles; Tween-NPs, Tween® 20-coated nanoparticles; Tf-R, transferrin receptor; PBCA, poly(butylcyanoacrylate); PBS-CMF, Ca^{2+}/Mg^{2+} free phosphate-buffered saline; Pe, endothelial permeability coefficient; PLA, poly(lactide); PLGA, poly(D,L-lactide-*co*-glycolide); RES, reticuloendothelial system; RH, Ringer–Hepes buffer; TEM, transmission electron microscopy.

* Corresponding author at: EA 2689, Laboratory of Physiology, IMPRT, University of Lille 2, Faculté de Médecine, pôle recherche, 1 place de Verdun, 59045 Lille, France. Tel.: +33 320626968; fax: +33 320626963.
E-mail address: dbetbeder@aol.com (D. Betbeder).

0378-5173/$ – see front matter © 2009 Elsevier B.V. All rights reserved.
doi:10.1016/j.ijpharm.2009.04.035

followed by receptor-mediated endocytosis of the particles by the brain capillary endothelial cells (BCECs) (Kreuter et al., 2002; Kim et al., 2007). This hypothesis was supported by the finding that covalent coupling of apolipoprotein E or A-1 to human serum albumin nanoparticles (HSA NPs) leads to similar effects (Michaelis et al., 2006; Petri et al., 2007; Kreuter et al., 2007).

The polyester poly(D,L-lactide-*co*-glycolide) (PLGA) NPs have also been studied for CNS drug delivery (Costantino et al., 2006), based on the characteristics of this material: PLGA is a biodegradable polymer, approved for human use by U.S. FDA, and decomposing without any induction of inflammation or immune reactions (Dechy-Cabaret et al., 2004). NPs made of PLGA conjugated with glyco-heptapeptides were already shown to cross the BBB after *in vivo* administration (Costantino et al., 2006).

Specific receptors of the brain capillary endothelium were identified for LDL (Dehouck et al., 1997), insulin (Frank et al., 1986), lactoferrin (Fillebeen et al., 1999), insulin-like growth factors (IGF-I and IGF-II) (Duffy and Pardridge, 1987), interleukin-1 (IL-1), folic acid (FA) (Wu and Pardridge, 1999) and transferrin (Tf) (Descamps et al., 1996). These receptors can be targeted with suitable ligands. Receptor-mediated transcytosis was illustrated for insulin, transferrin, LDL, lactoferrin and melanotransferrin (Duffy and Pardridge, 1987; Descamps et al., 1996; Dehouck et al., 1997; Fillebeen et al., 1999; Demeule et al., 2002). Tf receptor-mediated endocytosis is an efficient cellular uptake pathway for anticancer drugs delivery (Visser et al., 2004). The transferrin receptor (Tf-R) is overexpressed in many tumors (Högemann-Savellano et al., 2003) and has been widely studied. Tf or antibodies (for instance, R17217 and OX26 monoclonal antibody) against the Tf-R have been investigated in a number of studies (Boado et al., 1998; Aktaş et al., 2005). The aim of this study was to evaluate the brain endothelial cells targeting of PLGA NPs with transferrin, and the mechanisms involved in their endocytosis. Studies were performed with an *in vitro* model of BBB made of a *co*-culture of endothelial cells and astrocytes.

2. Materials and methods

2.1. Materials

PLGA (50:50, Resomer® RG 503H; Mw = 26,500 g/mol; Mn = 14,700 g/mol) was purchased from Boehringer Ingelheim (Germany). Fluorescent dyes 1,1′-dioctadecyl 3′,3,3′,3′-tetramethylindo-carboxycyanate perchlorate (DiI) and 5-([4,6-dichlorotriazin-2-yl]amino) fluorescein (FITC), Lucifer Yellow (paracellular marker), bovine serum albumin (BSA), FITC–BSA conjugant, human *holo*-transferrin (diferric Tf) (≥98%), Tween® 20, filipin and indomethacin (caveolae-mediated endocytosis inhibitors), chlorpromazine (clathrin-mediated endocytosis inhibitor) and NaN_3 (energy inhibitor) were from Sigma Chemical Co. (Saint Louis, MO). $^{[U\text{-}14C]}$sucrose (677 mCi/mmol) (paracellular marker) was obtained from Amersham Laboratories (Les Ulis, France). Deionized water and sterile water for injection were used throughout the experiment. All other chemicals used were of reagent grade. Sephadex G25 column (PD 10) was purchased from Amersham, Orsay, France. Bovine brain capillary endothelial cells (BCECs) were isolated and characterized as described by Meresse et al. (1989). Ringer–Hepes buffer (RH, pH = 7.4) contains 1.8 mM $CaCl_2$, 5.6 mM KCl, 0.8 mM $MgSO_4$, 0.8 mM NaH_2PO_4, 116 mM NaCl, 25 mM Hepes and 5.5 mM D-glucose; phosphate-buffered saline (PBS) is composed of 150 mM NaCl, 2.7 mM KCl, 1.3 mM KH_2PO_4 and 1 mM $Na_2HPO_4{\cdot}7H_2O$, pH 7.4; bicarbonate buffer 0.1 M, pH 9.5 is obtained by mixing a $NaHCO_3$ solution at 0.1 M with a Na_2CO_3 solution at 0.1 M to obtain a final solution at pH 9.5.

2.2. Methods

2.2.1. Preparation of NPs

Blank NPs and Tween–NPs were obtained by a modified solvent diffusion (nanoprecipitation) technique (Barichello et al., 1999). Briefly, PLGA (10 mg) was solubilized in acetone (850 μL), then 150 μL ethanol (97%) was added. This organic phase was quickly poured in 10 mL deionized water with/without 0.5% Tween® 20 (aqueous phase) under magnetic stirring at 1000 rpm for 3 h. Fluorescent NPs were prepared using the same protocol, DiI was added in the acetone solution of PLGA. The produced suspensions were then kept at 4 °C after filtration through 0.22-μm filter.

2.2.2. Preparation of FITC-labelled transferrin

FITC labelling of human *holo*-Tf was performed as described: human *holo*-Tf (25 μM) was dissolved in 0.1 M bicarbonate buffer, pH 9.5. 5-([4,6-dichlorotriazin-2-yl]amino) fluorescein (FITC) was first dissolved in 20 μL DMSO and then 980 μl of PBS was added to obtain a 125 μM FITC solution. This FITC solution was added dropwise into Tf solution with gentle stirring. After 6 h incubation at room temperature in the dark, uncoupled FITC was removed using a Sephadex G25 column equilibrated with PBS, and the labelled Tf was dialyzed against PBS at 4 °C. The FITC–Tf solution could be stored for 1 month at 4 °C.

2.2.3. Preparation of protein-coated NPs

Protein (transferrin or bovine serum albumin) was dissolved in Ringer–Hepes buffer (RH, pH 7.4) at a concentration of 1 mg/mL. Blank NPs were added to the protein solution at the ratio 1/1 (w/w). The adsorption reaction was left for 3 h at room temperature, with moderate shaking (Ataman-Onal et al., 2006).

The average quantity of protein adsorbed to NPs was calculated indirectly by measuring the amount of protein that was not conjugated to NPs. For this purpose, FITC-labelled protein (FITC-protein) was used. The products were centrifuged at 13,000 × *g* for 30 min and the suspension was collected to determine the amount of protein that did not bind to NPs according to a standard curve of FITC-protein, using a spectrofluorometer Fluoroskan Ascent FL (Thermo labsystemes) set at λ_{ex} = 425 nm and λ_{em} = 538 nm. Protein binding stability at 37 °C was assessed at different time intervals.

The average number of protein molecules conjugated per nanoparticle was calculated by dividing the number of proteins bound to NPs by the calculated average number (n) of NPs using the following equation (Sahoo et al., 2004):

$$n = \frac{6m}{\pi \times D^3 \times \rho}$$

where m is the NPs weight, D is the number based on mean NPs diameter determined by nanosizer and ρ = NPs weight per volume unit (density), estimated to be 1.1 g/cm^3 based on the polymer density.

2.2.4. Characterization of NPs

The particles size and size distribution of NPs were measured by N4 PLUS, Submicron Particle Size Analyzer (BECKMAN COULTER, N4 Plus software). Before measurement, the particle suspension was diluted by PBS (pH 7.4). The samples were examined for the mean particle diameter and poly-dispersity. The reported value is mean ± S.D. (n = 3). NPs surface charge was investigated through zeta potential measurements in 15 mM NaCl (Zetasizer 4, with a multi-8 correlator 7032, Malvern Instruments).

The morphology of NPs was examined by transmission electron microscopy (TEM) following negative staining with sodium phosphotungstate solution (0.2%, w/v) (Ruben et al., 2005). A drop of the sample was placed onto a carbon-coated copper grid to create a thin film. Before the film dried on the grid, it was negatively

stained with phosphotungstic acid by adding a drop of the staining solution to the film; any excess solution was drained off with a filter paper. The grid was allowed to dry, and samples were viewed under a transmission electron microscope (JEOL-100CX-II, Tokyo, Japan).

2.2.5. Cell culture and cellular studies

2.2.5.1. Preparation of filters for co-culture. Culture plate inserts (Transwell® 0.4-μm pore size, 4.67 cm^2 growth surface area; Corning Incorporated) were coated on the upper side with 150 μL of a 2 mg/mL solution of rat tail collagen containing 10-fold concentrated DMEM plus 0.3 M NaOH. The coated inserts were dried for 1 h at 37 °C and were rinsed twice with water and once with PBS-CMF (PBS, pH = 7.4; Ca^{2+}, Mg^{2+} free) before being placed in complete medium.

2.2.5.2. Brain capillary endothelial cells. Cell culture was performed according to Dehouck et al. (1992). Briefly, BCECs were isolated and characterized as described by Meresse et al. (1989). The endothelial cells were cultured in the presence of DMEM supplemented with 10% (v/v) heat inactivated calf serum and 10% (v/v) horse serum (Invitrogen), 2 mM glutamine, 50 μg/mL gentamicin, and basic fibroblast growth factor (1 ng/mL, added every other day).

2.2.5.3. Glial cells and co-culture of BCECs. Primary cultures of mixed glial cells composed of 60% astrocytes, 20% oligodendrocytes, and 20% microglia were prepared from newborn rat cerebral cortex. After removing the meninges, the brain tissue was forced gently through a nylon sieve, as described by Booher and Sensenbrenner (1972). Glial cells were plated on six-well plates at a concentration of 1.2×10^5 cells/mL in 2 mL of DMEM supplemented with 10% (v/v) fetal calf serum (Invitrogen), and the medium was changed twice a week. Three weeks after seeding, cultures of glial cells were stabilized and used for *co*-culture. Coated filters were set in six-well plates containing glial cells. Endothelial cells were plated on their upper side in 1.5 mL of medium at a concentration of 4×10^5 cells/mL. The *co*-culture medium was the same as that for BCECs. Under these conditions, BCECs formed a confluent monolayer after 7 days. Experiments were performed 5 days after confluence.

2.2.6. Membrane binding of nanoparticles at 4 °C

Prior to endocytosis studies, the luminal and abluminal side of the *co*-culture were washed twice with cold RH solution. Once filters containing endothelial cells were transferred into six-well plates containing RH solution (2.5 mL in abluminal side), RH solution (1.5 mL) containing 120 μg of NPs was placed, at time 0, in the upper compartment (luminal side). The incubations were performed at 4 °C. After 60 min, the quantity of NPs binding on BBB endothelial cells was calculated indirectly by measuring the amount of NPs in luminal side. The quantity of NPs was determined by spectrofluorometer Fluoroskan Ascent FL (Thermo labsystemes) set at λ_{ex} = 544 nm and λ_{em} = 590 nm.

2.2.7. Endocytosis studies of nanoparticles at 37 °C

For NPs uptake study, the experiments were performed at 37 °C in humified atmosphere with 5% CO_2. The luminal and abluminal sides of the *co*-culture were rinsed twice with RH and the inserts containing BCECs were transferred into six-well plates containing RH (2.5 mL in abluminal side). RH (1.5 mL) containing 120 μg of NPs was placed, at time 0, in the upper compartment (luminal side). At different time intervals, the inserts were transferred to the other wells to minimize the possibility of passage from the lower compartment. For each condition, three inserts were assayed. The quantity of NPs was determined as described above.

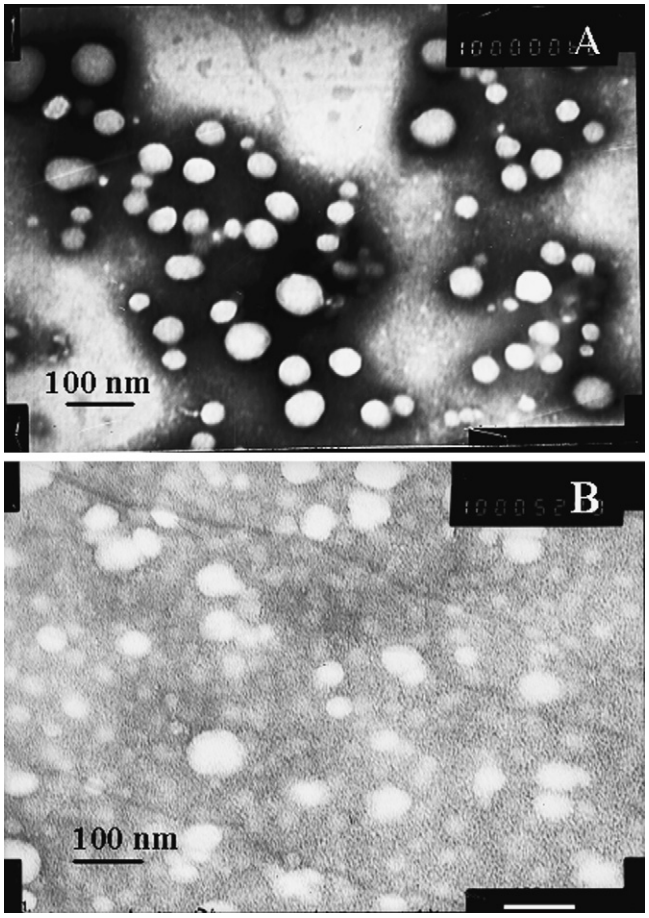

Fig. 1. TEM of (A) Blank NPs and (B) Tf-NPs (100×, 000), Bar =100 nm.

2.2.8. Transferrin receptor-mediated endocytosis

To examine the specificity of Tf receptor (Tf-R) mediated uptake of Tf-NPs, cells were incubated for 5 min with 150-times over concentration of free human *holo*-Tf (1.5 mg/mL) prior to incubation with 120 μg of Tf-NPs (i.e. 10 μg Tf were coated on NPs). The excess free Tf was incubated with the cells throughout the experiment. Particle uptake was analysed as mentioned above.

2.2.9. Endocytosis inhibitors treatment

The BCECs were first pretreated with inhibitors (10 μg/mL filipin, 10 μg/mL chlorpromazine, 10 μg/mL indomethacin, or 2 μg/mL NaN_3) for 15 min at 37 °C in humified atmosphere with 5% CO_2.

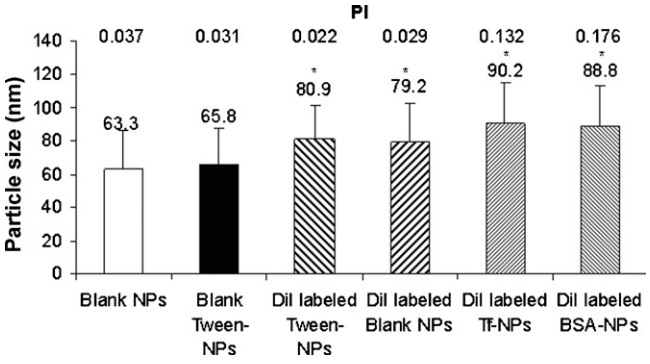

Fig. 2. Particle size of PLGA NPs (nm). (□) Blank NPs; (■) Blank Tween-NPs; (▨) DiI labelled Tween-NPs; (▨) DiI labelled Blank NPs; (▨) DiI labelled Tf-NPs; (▨) DiI labelled BSA-NPs. *$p < 0.05$ compared to Blank NPs (data as mean ± S.D.; $n = 3$).

Table 1
Zeta potential of PLGA NPs (mV).

Samples	Zeta potential (mV)
Blank NPs	−42.6 ± 6.6
Blank Tween-NPs	−22.7 ± 5.1*
BSA-NPs	−33.4 ± 7.8*
Tf-NPs	−31.9 ± 7.9*
Dil labelled Blank-NPs	−44.2 ± 8.9
Dil labelled Tween-NPs	−21.4 ± 7.3*
Dil labelled BSA-NPs	−33.1 ± 7.7*
Dil labelled Tf-NPs	−32.5 ± 8.2*

Data as mean ± S.D.; $n = 3$.
* $p < 0.05$.

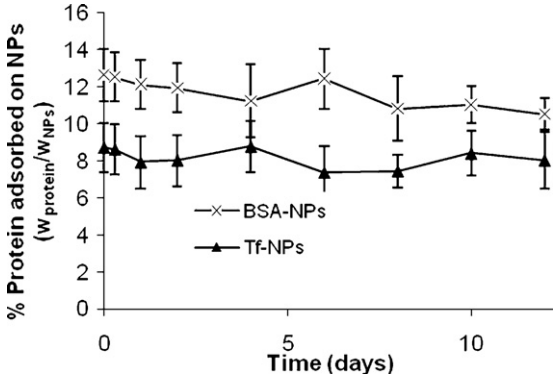

Fig. 3. Evaluation of the stability of protein adsorbed on surface of NPs in RH at 37 °C. At different time intervals, NPs were centrifuged and the amount of protein adsorbed on NPs was evaluated (data as mean ± S.D.; $n = 3$).

Then the cells were washed with RH and 120 μg of NPs was added. Endocytosis studies of NPs were analysed as described above.

2.2.10. Fluorescence microscopy

After NPs incubation, the cells were washed twice with RH solution followed with twice washing with 2% BSA solution and finally twice washing with RH solution at 4 °C. BCECs were fixed with 4% paraformaldehyde in PBS-CMF at room temperature. The filters and their attached monolayers were mounted on glass microscope slides with Mowiol mountant (Hoechst, Frankfurt, Germany), and the specimens were visualized and photographed with fluorescence microscope (Leica, Wetzlar, Germany). The photographs corresponding to each condition were analysed with SigmaScan

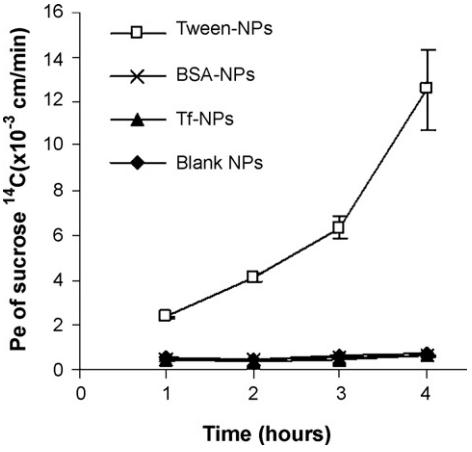

Fig. 4. Cytotoxicity studies: $^{[14C]}$sucrose Pe of cells incubated at different time intervals with Tween-NPs, BSA-NPs, Tf-NPs and Blank NPs (data as mean ± S.D.; $n = 3$).

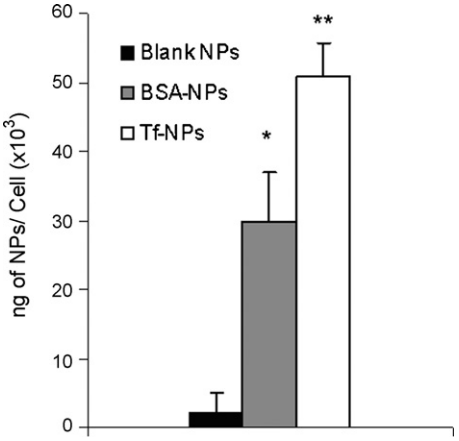

Fig. 5. Evaluation of endocytosis of NPs on BBB endothelial cells at 37 °C (nanogram of NPs/cell × 10^3, Lucifer Yellow Pe <1 for every experiment). (■) Blank NPs; (▩) BSA-NPs; (□) Tf-NPs. $^{**}p < 0.005$, $^{*}p < 0.05$. Tf-NPs vs. Blank NPs, or BSA-NPs vs. Blank NPs (data as mean ± S.D.; $n = 3$).

Software (Jandel Scientific, San Rafael, CA) to compare the different NPs endocytosis by BCECs.

2.2.11. Cytotoxicity assay

Paracellular passage was evaluated using either Lucifer Yellow (LY) or $^{[14C]}$sucrose at each time point. For each experiment, LY or $^{[14C]}$sucrose was used, as paracellular markers, in *co*-incubation with the tested compounds allowing the evaluation of the compound effect on the integrity of the BBB. They were added in the upper compartment containing the different test NPs. At each time of the experiments, aliquots were taken from each lower compartment. The amounts of LY in the lower compartment throughout the experiment were measured using a spectrofluorometer Fluoroskan Ascent FL (Thermo labsystemes) set at $\lambda_{ex} = 425$ nm and $\lambda_{em} = 538$ nm. Radiotracer concentration in the lower compartment was measured in a liquid scintillation counter (Wallac 14110; Pharmacia, Piscataway, NJ). The endothelial permeability coefficient (Pe in cm/min) was calculated as previously described (Dehouck et al.,

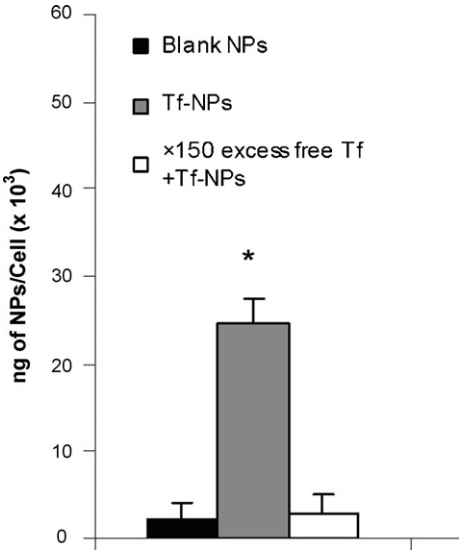

Fig. 6. Evaluation of endocytosis of Tf-NPs on BBB endothelial cells pre-incubated with excess free Tf at 37 °C. (Lucifer Yellow Pe <1 for every experiment). (■) Blank NPs; (▩) Tf-NPs; (□) Tf-NPs to cells pre-incubated with 100-times free Tf; $^{*}p < 0.005$, Tf-NPs vs. Tf-NPs to cells pre-incubated with 100-times free Tf, or Blank NPs (data as mean ± S.D.; $n = 3$).

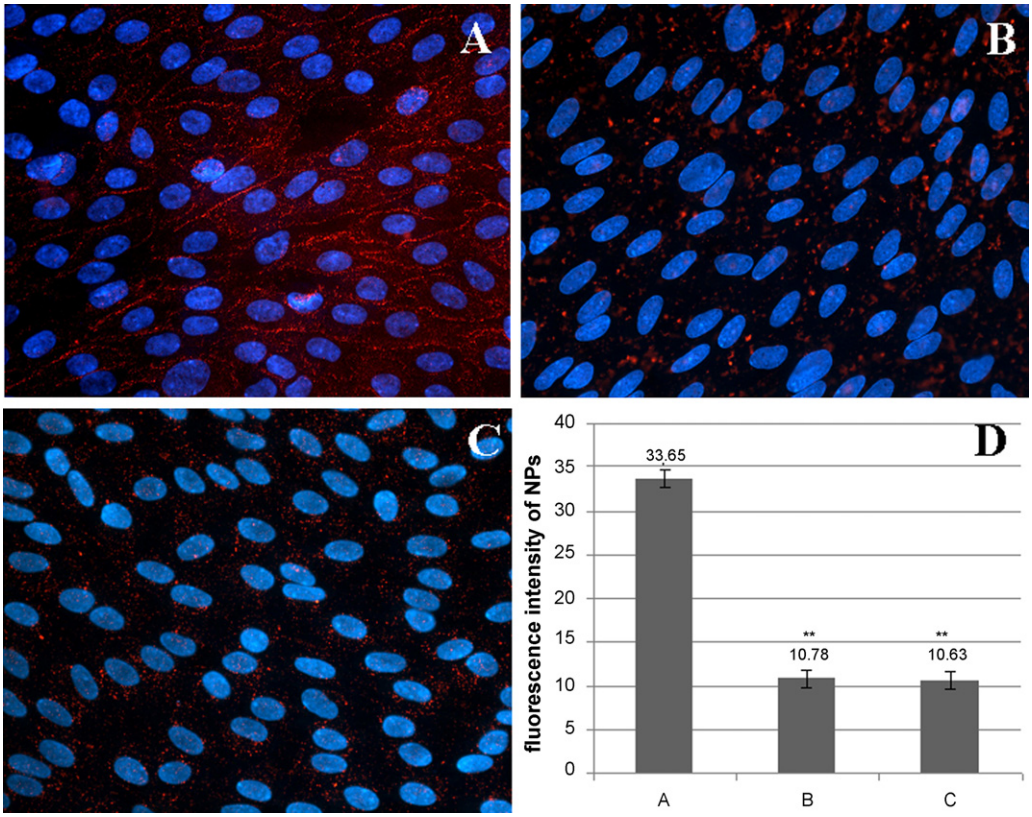

Fig. 7. Fluorescence microscopy of Tf-NPs endocytosis on BBB endothelial cells after 1 h (A) at 37 °C, (B) at 4 °C and (C) at 37 °C cells pre-incubated with excess free Tf; (D) fluorescence intensity analysis of DiI-NPs in (A)–(C) by SigmaScan software (data as mean ± S.D.; $n = 3$), $^{**}p < 0.005$. The cells nuclei are stained with Hoechst and the NPs are labelled with DiI (Lucifer Yellow Pe <1 for every experiment).

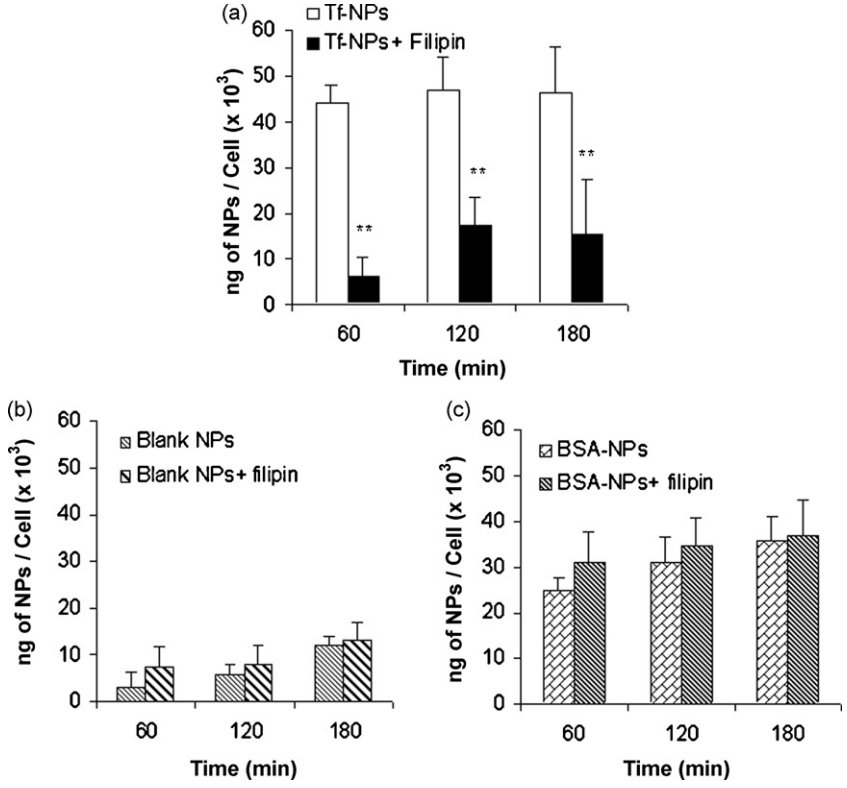

Fig. 8. Kinetics of NPs endocytosis by BBB endothelial cells pretreated or not by filipin (Lucifer Yellow Pe <1 for every experiment). (a) Tf-NPs; (b) Blank NPs; (c) BSA-NPs (data as mean ± S.D.; $n = 3$), $^{**}p < 0.005$.

1992). Only experiment values where Pe of [14C]sucrose or LY were $<1 \times 10^{-3}$ cm/min was taken into account.

2.2.12. Statistical analysis

One-way analyses of variance (ANOVA) test was performed on the data to assess the impact of the formulation variables on the results ($n = 3$). $p < 0.05$ was considered significant. All calculations were performed using a statistical software program (SPSS® 11.5, Microsoft).

3. Results

3.1. Nanoparticle characterization

We prepared NPs using the solvent diffusion technique in presence or absence of Tween® 20. Transmission electron microscopy showed that the NPs are almost spheric in shape (Fig. 1). Size distribution of all particles was unimodal with a mean diameter of 63–90 nm (Fig. 2). DiI incorporation in NPs increased their mean hydrodynamic diameter from 63 to 79 nm while the use of Tween® 20 did not inhibit this phenomenon. Furthermore, as expected, a further increase was observed when proteins were adsorbed on their surface. The zeta potential of Blank NPs decreases when Tween® 20, BSA or Tf coated the NPs (Table 1). DiI labelling did not affect their zeta potential.

3.2. Stability studies

Short term size stability of the particles was evaluated at 4 and 37 °C (data not shown). No size increase was observed at 4 °C for 28 days while at 37 °C only Blank NPs slowly aggregated after 8 days incubation. Blank NPs prepared without Tween® 20 were colloidally unstable and rapidly coalesced (Jain, 2000).

We followed the stability of protein adsorption on NPs at 37 °C in RH. No protein desorption was observed even after 12 days incubation (Fig. 3). To quantify the endocytosis of NPs by the endothelial cells, we used the fluorescent dye (DiI) as lipophilic marker. High fluorescence stability of DiI was found even after one week incubation at 37 °C in RH due to no change of fluorescence intensity of NPs (data not shown). To further confirm this result, NPs were centrifuged at 13,000 × *g* for 30 min and NPs were then recovered in suspension and passed through 0.22-μm filter. No DiI was lost during this process, contrary to free DiI which could not be filtered.

The amount of protein conjugated to NPs was 126 μg BSA/mg NPs, and 89 μg Tf/mg NPs, which represents approximately 443 BSA molecules per nanoparticle, and 268 Tf molecules per nanoparticle.

3.3. Cytotoxicity studies

Strong toxicity was observed for Tween–NPs as [14C]sucrose paracellular passage dramatically increased ([14C]sucrose Pe $>2 \times 10^{-3}$ cm/min after 1 h incubation compared to 0.2×10^{-3} cm/min for other NPs) (Fig. 4). Similar toxicity results with another surfactant (polysorbate 80) were already described (Olivier et al., 1999). For all the other studies in this paper, Tween® 20 was not used, and the Pe of the [14C]sucrose or Lucifer Yellow (paracellular markers to BBB) was always <1.

3.4. Nanoparticle endocytosis by endothelial cells

Cellular endocytosis of Tf-NPs was about 20-fold greater than Blank NPs and 2-fold greater than BSA-NPs (Fig. 5) while no toxicity was observed as no increase of paracellular passage of LY was observed. The specificity of receptor-mediated endocytosis of Tf-NPs was evident from the reduced endocytosis when endothelial cells were pre-incubated with 150-times free Tf (compared to Tf on NPs) (Fig. 6). Further, the level of endocytosis of Tf-NPs in the presence of large excess free Tf was similar to that of Blank NPs. The higher cellular uptake is due to higher intracellular delivery (Fig. 7). Experiments performed at 37 °C show that Tf-NPs were found in microvesicles (Fig. 7A), while at 4 °C they have a homogenous distribution and a low endocytosis by BCECs (Fig. 7B). Lower endocytosis is observed when cells are incubated with 150-times concentrated free Tf (Fig. 7C). Quantitative analysis according to fluorescence intensity of DiI labelled NPs confirmed that the endocytosis of NPs was inhibited by low temperature and Tf-R saturation (Fig. 7D). All these results suggest that Tf-NPs interact with BBB in a specific manner that facilitates their endocytosis.

3.5. Mechanism of NPs endocytosis

Filipin, a caveolae inhibitor known to bind cholesterol and disorganize caveoale (Severs, 1997) was found to inhibit nanoparticle uptake while no significant effect was observed either with Blank NPs or BSA-NPs (Fig. 8). This result suggests that Tf-NPs contrary to Blank NPs or BSA-NPs are endocytosed via a cholesterol dependent pathway. Fluorescence microscopy showed that few Tf-NPs are found when cells are pretreated with filipin (Fig. 9A). Further

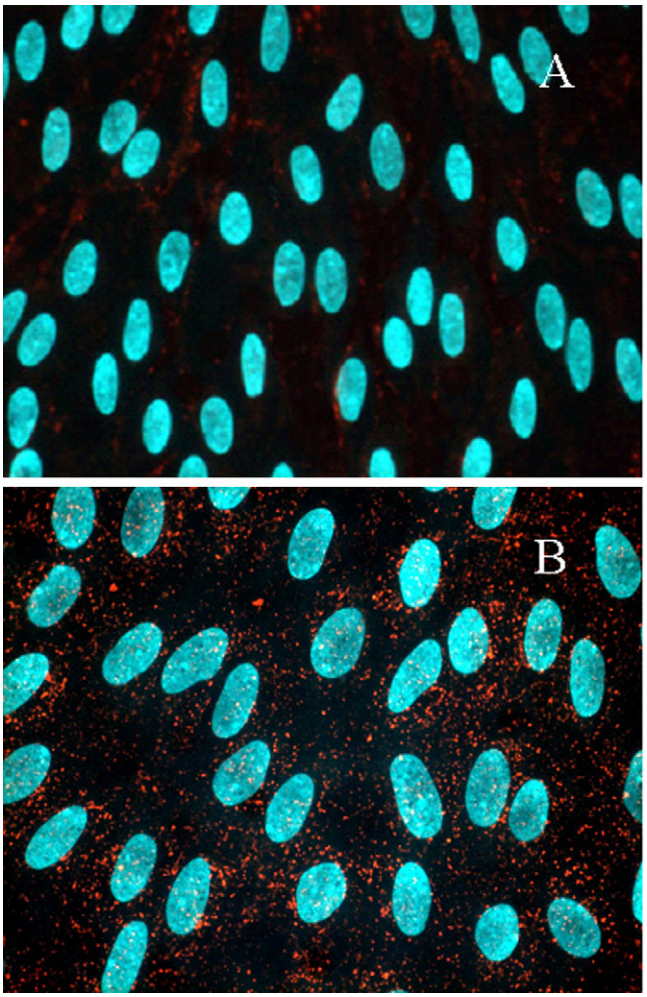

Fig. 9. Fluorescence microscopy of Tf-NPs endocytosis on BBB endothelial cells, after 60 min incubation with (A) and without (B) pretreatment with filipin. The cell nuclei are stained with Hoechst and the NPs are labelled with DiI (Lucifer Yellow Pe <1 for every experiment).

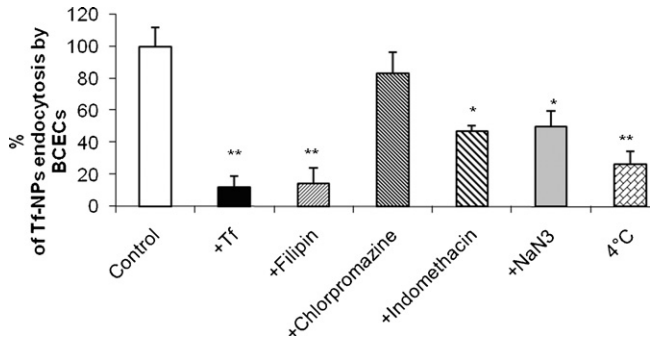

Fig. 10. Evaluation of Tf-NPs endocytosis on BBB endothelial cells after 1 h incubation (Lucifer Yellow Pe <1 for every experiment). (□) Control; (■) cells pretreated with free *holo*-transferrin; (▨) cells pretreated with filipin; (▨) cells pretreated with chlorpromazine; (▨) cells pretreated with indomethacin; (■) cells pretreated with NaN_3; (▨) cells incubated at 4 °C; (data as mean ± S.D.; $n = 3$) $^{**}p < 0.005$, cells pretreated with Tf, filipin, incubated at 4 °C vs. control at 37 °C; $^{*}p < 0.05$, cells pretreated with indomethacin, or NaN_3 at 37 °C vs. control at 37 °C.

studies performed using different types of inhibitors or treatments including clathrin and caveolae inhibitors also confirmed this previous result (Fig. 10). The results show that NPs endocytosis is lowered when the treatments were performed at 4 °C, or in presence of sodium azide (NaN_3), which suggested that their endocytosis is energy dependent. Furthermore, indomethacin, known to inhibit caveolae pathway, significantly inhibited particle endocytosis while chlorpromazine had no effect.

4. Discussion and conclusion

To evaluate NPs endocytosis by the BBB, we developed an *in vitro* model based on a *co*-culture of brain endothelial and glial cells. This *co*-culture retains all endothelial cell markers and the characteristics of the blood–brain barrier, including tight junctions, γ-glutanyl transpeptidase (γ-GT) activity and receptors such as LDL receptor and Tf receptor (Dehouck et al., 1997; Cecchelli et al., 2007). A good *in vitro–in vivo* correlation was obtained in this model suggesting that it is relevant for investigating the role of the BBB in drug delivery to the brain (Dehouck et al., 1992; Lundquist et al., 2002).

NPs formulated from PLGA polymer offer a non-toxic and efficient carrier system for the delivery of drugs within the cells (Weissenböck et al., 2004). The aggregation of PLGA NPs during solvent evaporation process is a notable problem regardless of the different preparation methods. In order to prevent PLGA NPs aggregation, polymer stabilizers are often used. Many stabilizers such as poly (vinyl alcohol) (PVA) (Abdelwahed et al., 2006), poly (vinyl pyrrolidone), Tween® 80 (Alyautdin et al., 1997) are excellent stabilizer candidates. These stabilizers are coated on the surface of PLGA NPs and prevent NPs aggregation. However they are difficult to be removed even through thorough washing and some of them can be toxic to the blood–brain barrier (Olivier et al., 1999). Furthermore, in our studies, Tween® 20 was also found to be toxic (Fig. 4). To avoid this problem we found that protein adsorption (BSA or Tf) without the use of detergent was able to coat these NPs in a stable manner and increase their stability at 37 °C. Furthermore, this process avoids the use of chemical reactants and organic solvent, which can induce potentially partial loss of protein conformation. Tf-coated NPs were characterized in terms of size, zeta potential (Table 1) and protein binding analysis (Figs. 2 and 3). We observed that zeta potential of NPs coated with proteins decreased significantly. Moreover, their binding on the NPs surface was stable for at least 12 days at 37 °C. Meanwhile, we found surface coating of NPs with Tf allowed effective targeting of BBB by 20-fold increase (Fig. 5). The binding of Tf (determined at 4 °C) was approximately 4-fold lower than the association at 37 °C (Fig. 4D, Fig. 10), indicating that endocytosis took place via an active process. Fig. 6 shows that the endocytosis of Tf-NPs was inhibited by 150-times excess free Tf, suggesting that Tf-NPs were selectively endocytosed. Schnitzer et al. (1994) have shown that filipin, a macrolide antibiotic that binds sterols and then causes disassembly of caveolae, reduces transcellular transport of insulin across endothelial cell monolayers where it does not inhibit insulin endocytosis for degradation. Studies involving a short treatment with filipin on endocytosis of FITC–Tf showed that the effect of filipin is reversible, and thus, the fundamental functions of endothelial cells are not altered by filipin treatment (Cecchelli et al., 2007). This also suggests that caveolae is likely to be involved in the potential transport of Tf-NPs from the blood to the brain.

Here, we investigated the protein-NPs and Blank NPs intracellular routing at the brain capillary endothelial cell level. The pretreatment of endothelial cells with filipin results in the total inhibition of Tf-NPs, but not for Blank NPs or BSA-NPs (Fig. 8). Moreover, chlorpromazine known to dissociate clathrin-coated vesicles from the plasma membrane, had no effect on the Tf endocytosis within endothelial cells. These results suggest that a caveolae endocytosis pathway is preferentially involved in Tf-NPs and traffic within the endothelial cells. The endocytosis of Blank NPs or BSA-NPs occurred probably by a non-specific process, that is, adsorptive mediated endocytosis (Bickel et al., 2001).

Caveolae-mediated transcytosis of Tf was shown in the *in vitro* model of *co*-culture of endothelial cells and astrocytes (Balazs et al., 2004; Cecchelli et al., 2007; Candela et al., 2008). However in other models of culture, the endocytosis was described using the clathrin pathway (Visser et al., 2004). These results clearly show the complexity of the blood–brain barrier.

Particles in the nanometer range have easy accessibility in the body, being transported to different parts of the body via the blood circulation. Particles less than 100 nm diameter with hydrophilic surface, have been found to have longer circulation in blood (Moghimi et al., 2001). The interaction of the colloidal carriers with blood plasma proteins (opsonins) and with the membranes of macrophages (opsonization) is believed to be the major criteria for the clearance of these drug delivery systems from the bloodstream or allows brain specific targeting via apolipoprotein E adsorption (Kim et al., 2007). Further studies are planned to evaluate: blood protein binding to these NPs coated with Tf; their biodistribution after *in vivo* administration, and treatment of glioma in rats using drug carried Tf-NPs formulations.

Acknowledgments

This work is supported by grants from the PhD fellowship between France and China from the French Research Ministry. We would like to thank Pr R. Cecchelli and all the members of the Laboratory of Blood-brain Barrier for their help during the cell culture and for scientific advice, in particular Pr L. Fenart and Pr M.P. Dehouck.

References

Abdelwahed, W., Degobert, G., Fessi, H., 2006. A pilot study of freeze drying of poly(epsilon-caprolactone) nanocapsules stabilized by poly(vinyl alcohol): formulation and process optimization. Int. J. Pharm. 309, 178–188.

Aktaş, Y., Yemisci, M., Andrieux, K., Gürsoy, R.N., Alonso, M.J., Fernandez-Megia, E., Novoa-Carballal, R., Quiñoá, E., Riguera, R., Sargon, M.F., Celik, H.H., Demir, A.S., Hincal, A.A., Dalkara, T., Capan, Y., Couvreur, P., 2005. Development and brain delivery of chitosan–PEG nanoparticles functionalized with the monoclonal antibody OX26. Bioconjug. Chem. 16, 1503–1511.

Alyautdin, R.N., Petrov, V.E., Langer, K., Berthold, A., Kharkevich, D.A., Kreuter, J., 1997. Delivery of loperamide across the blood–brain barrier with polysorbate 80-coated polybutylcyanoacrylate nanoparticles. Pharm. Res. 14, 325–328.

Ambruosi, A., Khalansky, A.S., Yamamoto, H., Gelperina, S.E., Begley, D.J., Kreuter, J., 2006. Biodistribution of polysorbate 80-coated doxorubicin-loaded $^{[14C]}$-

poly(butyl cyanoacrylate) nanoparticles after intravenous administration to glioblastoma-bearing rats. J. Drug Target. 14, 97–105.
Ataman-Onal, Y., Munier, S., Ganée, A., Terrat, C., Durand, P.Y., Battail, N., Martinon, F., Le Grand, R., Charles, M.H., Delair, T., Verrier, B., 2006. Surfactant-free anionic PLA nanoparticles coated with HIV-1 p24 protein induced enhanced cellular and humoral immune responses in various animal models. J. Control. Release 112, 175–185.
Balazs, Z., Panzenboeck, U., Hammer, A., Auehenberger, O., Malle, E., Sattler, W., 2004. Uptake and transport of high-density lipoprotein (HDL) and HDL-associated atocopherol by an in vitro blood–brain barrier model. J. Neurochem. 89, 939–950.
Barichello, J.M., Morishita, M., Takayama, K., Nagai, T., 1999. Encapsulation of hydrophilic and lipophilic drugs in PLGA nanoparticles by the nanoprecipitation method. Drug Dev. Ind. Pharm. 25, 471–476.
Bickel, U., Yoshikawa, T., Pardridge, W.M., 2001. Delivery of peptides and proteins through the blood–brain barrier. Adv. Drug Deliv. 46, 247–279.
Blasi, P., Giovagnoli, S., Schoubben, A., Ricci, M., Rossi, C., 2007. Solid lipid nanoparticles for targeted brain drug delivery. Adv. Drug Deliv. Rev. 59, 454–477.
Boado, R.J., Tsukamoto, H., Pardridge, W.M., 1998. Drug delivery of antisense molecules to the brain for treatment of Alzheimer's disease and cerebral AIDS. J. Pharm. Sci. 87, 1308–1315.
Booher, J., Sensenbrenner, M., 1972. Growth and cultivation of dissociated neurons and glial cells from embryonic chick, rat and human brain in flask cultures. Neurobiology 2, 97–105.
Calvo, J.P., Gouritin, B., Chacun, H., Desmaele, D., D'Angelo, J., Noel, J.P., Georgin, D., Fattal, E., Andreux, J.P., Couvreur, P., 2001. Long-circulating PEGylated polycyanoacrylate nanoparticles as new drug carrier for brain delivery. Pharm. Res. 18, 1157–1166.
Candela, P., Gosselet, F., Miller, F., Buee-Scherrer, V., Torpier, G., Cecchelli, R., Fenart, L., 2008. Physiological pathway for low-density lipoproteins across the blood–brain barrier: transcytosis through brain capillary endothelial cells in vitro. Endothelium 15, 254–264.
Cecchelli, R., Berezowski, V., Lundquist, S., Culot, M., Renftel, M., Dehouck, M.P., Fenart, L., 2007. Modeling of the blood–brain barrier in drug discovery and development. Nat. Rev. Drug Discov. 6, 650–661.
Costantino, L., Gandolfi, F., Bossy-Nobs, L., Tosi, G., Gurny, R., Rivasi, F., Vandelli, M.A., Forni, F., 2006. Nanoparticulate drug carriers based on hybrid poly(D,L-lactide-co-glycolide)-dendron structures. Biomaterials 27, 4635–4645.
Dechy-Cabaret, O., Martin-Vaca, B., Bourissou, D., 2004. Controlled ring-opening polymerization of lactide and glycolide. Chem. Rev. 104, 6147–6176.
Dehouck, M.P., Jolliet-Riant, P., Brée, F., Fruchart, J.C., Cecchelli, R., Tillement, J.P., 1992. Drug transfer across the blood–brain barrier: correlation between in vitro and in vivo models. J. Neurochem. 58, 1790–1797.
Dehouck, B., Fenart, L., Dehouck, M.P., Pierce, A., Torpier, G., Cecchelli, R., 1997. A new function for the LDL receptor: transcytosis of LDL across the blood–brain barrier. J. Cell Biol. 138, 877–889.
Demeule, M., Poirier, J., Jodoin, J., Bertrand, Y., Desrosiers, R.R., Dagenais, C., Nguyen, T., Lanthier, J., Gabathuler, R., Kennard, M., Jefferies, W.A., Karkan, D., Tsai, S., Fenart, L., Cecchelli, R., Béliveau, R., 2002. High transcytosis of melanotransferrin (P97) across the blood–brain barrier. J. Neurochem. 83, 924–933.
Descamps, L., Dehouck, M.P., Torpier, G., Cecchelli, R., 1996. Receptor-mediated transcytosis of transferrin through blood–brain barrier endothelial cells. Am. J. Physiol. 270, 1149–1158.
Duffy, K.R., Pardridge, W.M., 1987. Blood–brain barrier transcytosis of insulin in developing rabbits. Brain Res. 420, 32–38.
Edwards, R.T., 2001. Drug delivery via the blood–brain barrier. Nat. Neurosci. 4, 221–222.
Fillebeen, C., Descamps, L., Dehouck, M.P., Fenart, L., Benaïssa, M., Spik, G., Cecchelli, R., Pierce, A., 1999. Receptor-mediated transcytosis of lactoferrin through the blood–brain barrier. J. Biol. Chem. 274, 7011–7017.
Frank, H.J., Pardridge, W.M., Jankovic-Vokes, T., Vinters, H.V., Morris, W.L., 1986. Insulin binding to the blood–brain barrier in the streptozotocin diabetic rat. J. Neurochem. 47, 405–411.
Hawkins, B.T., Davis, T.P., 2005. The blood–brain barrier/neurovascular unit in health and disease. Pharm. Rev. 57, 173–185.
Högemann-Savellano, D., Bos, E., Blondet, C., Sato, F., Abe, T., Josephson, L., Weissleder, R., Gaudet, J., Sgroi, D., Peters, P.J., Basilion, J.P., 2003. The transferrin receptor: a potential molecular imaging marker for human cancer. Neoplasia 5, 495–506.
Huwyler, J., Wu, D., Pardridge, W.M., 1996. Brain drug delivery of small molecules using immunoliposomes. Proc. Natl. Acad. Sci. U.S.A. 93, 14164–14169.
Jain, R.A., 2000. The manufacturing techniques of various drug loaded biodegradable poly(lactide-co-glycolide) (PLGA) devices. Biomaterials 21, 2475–2490.
Kim, H.R., Andrieux, K., Gil, S., Taverna, M., Chacun, H., Desmaële, D., Taran, F., Georgin, D., Couvreur, P., 2007. Translocation of poly(ethylene glycol-co-hexadecyl)cyanoacrylate nanoparticles into rat brain endothelial cells: role of apolipoproteins in receptor-mediated endocytosis. Biomacromolecules 8, 793–799.
Kreuter, J., Shamenkov, D., Petrov, V., Ramge, P., Cychutek, K., Koch-Brandt, C., Alyautdin, R., 2002. Apolipoprotein-mediated transport of nanoparticle-bound drugs across the blood–brain barrier. J. Drug Target. 10, 317–325.
Kreuter, J., Hekmatara, T., Dreis, S., Vogel, T., Gelperina, S., Langer, K., 2007. Covalent attachment of apolipoprotein A-I and apolipoprotein B-100 to albumin nanoparticles enables drug transport into the brain. J. Control. Release 118, 54–58.
Lundquist, S., Renftel, M., Brillault, J., Fenart, L., Cecchelli, R., Dehouck, M.P., 2002. Prediction of drug transport through the blood–brain barrier in vivo: a comparison between two in vitro cell models. Pharm. Res. 19, 976–981.
Meresse, S., Dehouck, M.P., Delorme, P., Bensaid, M., Tauber, J.P., Delbart, C., Fruchart, J.C., Cecchelli, R., 1989. Bovine brain endothelial cells express tight junctions and monoamine oxidase activity in long-term culture. J. Neurochem. 53, 1363–1371.
Michaelis, K., Hoffmann, M.M., Dreis, S., Herbert, E., Alyautdin, R.N., Michaelis, M., Kreuter, J., Langer, K., 2006. Covalent linkage of apolipoprotein E to albumin nanoparticles strongly enhances drug transport into the brain. J. Pharm. Exp. Ther. 317, 1246–1253.
Moghimi, S.M., Hunter, A.C., Murray, J.C., 2001. Long-circulating and target-specific nanoparticles: theory to practice. Pharmacol. Rev. 53, 283–318.
Olivier, J.C., Fenart, L., Chauvet, R., Pariat, C., Cecchelli, R., Couet, W., 1999. Indirect evidence that drug brain targeting using polysorbate 80-coated polybutylcyanoacrylate nanoparticles is related to toxicity. Pharm. Res. 16, 1836–1842.
Petri, B., Bootz, A., Khalansky, A., Hekmatara, T., Müller, R., Uhl, R., Kreuter, J., Gelperina, S., 2007. Chemotherapy of brain tumour using doxorubicin bound to surfactant-coated poly(butyl cyanoacrylate) nanoparticles: revisiting the role of surfactants. J. Control. Release 117, 51–58.
Ricci, M., Blasi, P., Giovagnoli, S., Rossi, C., 2006. Delivering drugs to the central nervous system: a medicinal chemistry or a pharmaceutical technology issue? Curr. Med. Chem. 13, 1757–1775.
Ruben, G.C., Wang, J.Z., Iqbal, K., Grundke-Iqbal, I., 2005. Paired helical filaments (PHFs) are a family of single filament structures with a common helical turn period: negatively stained PHF imaged by TEM and measured before and after sonication, deglycosylation, and dephosphorylation. Microsc. Res. Tech. 67, 175–195.
Sahoo, S.K., Ma, W., Labhasetwar, V., 2004. Efficacy of transferrin-conjugated paclitaxel-loaded nanoparticles in a murine model of prostate cancer. Int. J. Cancer 112, 335–340.
Schnitzer, J.E., Oh, P., Pinney, E., Allard, J., 1994. Filipin-sensitive caveolae-mediated transport in endothelium: reduced transcytosis, scavenger endocytosis, and capillary permeability of select macromolecules. J. Cell Biol. 127, 1217–1232.
Severs, N.J., 1997. Cholesterol cytochemistry in cell biology and disease. Subcell. Biochem. 28, 477–505.
Tosi, G., Costantino, L., Rivasi, F., Ruozi, B., Leo, E., Vergoni, A.V., Tacchi, R., Bertolini, A., Vandelli, M.A., Forni, F., 2007. Targeting the central nervous system: in vivo experiments with peptide-derivatized nanoparticles loaded with loperamide and rhodamine-123. J. Control. Release 122, 1–9.
Visser, C.C., Stevanović, S., Heleen Voorwinden, L., Gaillard, P.J., Crommelin, D.J., Danhof, M., DeBoer, A.G., 2004. Validation of the transferrin receptor for drug targeting to brain capillary endothelial cells in vitro. J. Drug Target. 12, 145–150.
Weissenböck, A., Wirth, M., Gabor, F., 2004. WGA-grafted PLGA-nanospheres: preparation and association with Caco-2 single cells. J. Control. Release 99, 383–392.
Wu, D., Pardridge, W.M., 1999. Blood–brain barrier transport of reduced folic acid. Pharm. Res. 16, 415–419.